Journal of Molecular Structure 1037 (2013) 288–293

Contents lists available at SciVerse ScienceDirect

Journal of Molecular Structure

journal homepage: www.elsevier.com/locate/molstruc

Synthesis, structure, and one- and two-photon absorption properties of *N*-substituted 3,5-bisarylidene*propen*piperidin-4-ones

Evgeniya S. Leonova [a], Nikolay S. Makarov [b], Alexandr Fonari [a], Rachael Lucero [a], Joseph W. Perry [b], David M. Sammeth [a], Tatiana V. Timofeeva [a,*]

[a] New Mexico Highlands University, Las Vegas, NM 87701, USA
[b] School of Chemistry and Biochemistry and Center for Organic Photonics and Electronics, Georgia Institute of Technology, Atlanta, GA 30332, USA

HIGHLIGHTS

- A series of 3,5-bisarylidene*propen*piperidin-4-one compounds was synthesized as possible sensitizers for photodynamic therapy.
- Their potential applicability as photosensitizers was proved by measurements of their one- and two-photon absorption spectra.
- For two compounds TPA cross sections is at least six times larger than for earlier synthesized 3,5-bis(arylidene)piperidin-4-ones.
- Spectral data are discussed in connection with structural characteristics of studied materials.

ARTICLE INFO

Article history:
Received 2 November 2012
Received in revised form 17 December 2012
Accepted 17 December 2012
Available online 5 January 2013

Keywords:
3,5-Bis(arylidene)piperidin-4-one
One-photon absorption
Two-photon absorption

ABSTRACT

A series of 3,5-bisarylidene*propen*piperidin-4-one compounds with a D–π–A–π–D structure, containing donors ($R^1 = NEt_2$, NMe_2) and terminal groups at the central nitrogen ring atom (R^2 = H, Me, Et, $P(O)(OEt)_2$) was synthesized with the goal of improving one- and two-photon absorption properties of the earlier designed compounds, which potential activity as photosensitizers was demonstrated with appeal of biological and spectroscopic data. Several of the compounds studied have a two photon absorption cross section approximately six times larger than previously measured for 3,5-bisarylidene*methylen*piperidin-4-ones with short alkene chains. Spectral data are discussed in connection with structural characteristics of studied materials.

1. Introduction

For α,β-unsaturated ketones, the key position is occupied by 3,5-bis(arylidene)piperidinones [1,2]. There is significant interest in these molecules due to their noticeable affinity toward thiols in cells. This is observed both in vitro and in vivo with little or no affinity toward the hydroxyl and amino groups found in nucleic acids [3–5]. Previously these compounds have been shown to be Mannich bases due to the structure of the 1,5-diaryl-3-oxo-1,4-pentadienyl pharmacophore (Fig. 1, [1]blue line), which interacts with cellular constituents [6–8] and allows them to display selective toxicity to neoplasms but not to corresponding normal cells [9].

Initial studies of these compounds show their antitumor [10,11], antiviral [12], anti-tuberculosis [13] and anti-inflammatory activities [14]. In addition, it was found, that the presence of the strong electron donors in the 1,5-diaryl-3-oxo-1,4-pentadienyl pharmacophore converts 3,5-bis(arylidene)piperidinones into the compounds with considerable one- and two-photon absorptions and therefore possible sensitizers [15] for photodynamic therapy (PDT). In addition to appropriate light absorption characteristics, potential photosensitizers should exhibit high stability, absorption in the near IR region, high extinction coefficients and negligible photobleaching. Compounds which can be used for PDT currently include push–pull olefins [16], various porphyrin derivatives [17], conjugated polymers [18] and dendrimers [19]. 3,5-Bis(arylidene)piperidinones present a unique class of compounds to further investigations in the development of PDT sensitizers.

Based on quantum-chemical computations [20], it was suggested that molecules with elongated methylene chains between donor and acceptor group should manifest higher one-photon absorption (OPA) and two-photon absorption (TPA) properties and consequently higher phototoxic activity. Several such compounds were previously synthesized [15] and studied. These compounds demonstrated low fluorescence quantum yields and short fluorescence lifetime, suggesting that there might be significant

* Corresponding author.
E-mail address: tvtimofeeva@nmhu.edu (T. V. Timofeeva).

[1] For interpretation of color in Fig. 1, the reader is referred to the web version of this article.

0022-2860/$ - see front matter © 2013 Elsevier B.V. All rights reserved.
http://dx.doi.org/10.1016/j.molstruc.2012.12.034

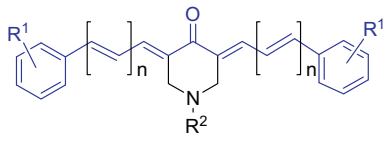

$(R^1Ph)_2prPR^2$

Fig. 1. General structure of the 3,5-bis(arylidene)piperidinones.

excited triplet state formation. Both dark cytotoxicity and phototoxicity toward A549 (lung), HepG2 (liver), Cal27 (tongue), MCF-7 (breast) and C4–2 (prostate) cancer cell lines were measured. The highest phototoxicity/cytotoxicity ratio was found for a compound with elongated methylene chain. These preliminary studies provided the direction and motivation for improving the photosensitive properties 3,5-bis(arylidene)piperidinones. As a continuation of the previous work here we present synthesis and characterization of substituted 3,5-bisarylidene*propen*piperidin-4-ones with general formula **$(R^1Ph)_2prPR^2$**, where **R^1** – donor groups attached to phenyl ring (R^1 = NEt_2, NMe_2), **R^2** – substituents at the N atom of the central acceptor piperidone core (R^2 = H, Me, Et, P(O)$(OEt)_2$), **P** – peperidone and ***pr*** – propene (n = 1), linker between donor and acceptor fragments (Fig. 1). This formula gives the foundational molecular structure and will be referenced in the discussions below. The spectroscopic and structural characteristics of all new materials are presented and discussed within the context of future applications.

2. Results and discussion

2.1. Chemistry

The synthesis of substituted 3,5-bisarylidene*propen*piperidin-4-ones **$(R^1Ph)_2prPR^2$** was carried out by earlier developed procedure utilizing aldol condensation between aldehydes **3a,b** and *N*-derivatives of piperidin-4-ones **1, 2a,b** [21] (Scheme 1). For a catalyst we used strong Lewis acid ($BF_3{\cdot}Et_2O$) in acetonitrile, which resulted in the products as BF_4 salts, facilitate the separation of desired products as clear solid material due to differences in solubility of the starting materials and the products. The salts were neutralized without further characterization. Derivatives of 3,5-bisarylidene*propen*piperidin-4-ones, **$(R^1Ph)_2prPR^2$**, were obtained with high yields presented in Scheme 1.

It is well known that the phosphorylation is used to improve drug delivery, as well as cytotoxicity [22]. The compound **$(Me_2NPh)_2prPP(O)(OEt)_2$** was synthesized (Scheme 2) to estimate phosphorus's influence on the properties of the these materials.

The *NH*— derivative of 3,5-bis(arylidene)piperidin-4-one **$(Me_2NPh)_2prPH$** was phosphorylated by diethyl chloridophosphate under basic conditions. Chloroform was chosen as solvent, providing good solubility of both starting material and product. As it turned out, the strength of triethylamine as a base was optimal for the transformation and resulted in a yield of 65%. The chemical structures of synthesized products were confirmed by NMR, mass-spectroscopy, IR and single crystal X-ray analysis.

2.2. Molecular and structural properties of 3,5-bisarylidenepropenpiperidin-4-ones

Of the series of synthesized compounds we were able to crystallize one of them **$(Me_2NPh)_2prPEt$** using methylene chloride and diethyl ether (slow diffusion). Structural characterization of **$(Me_2NPh)_2prPMe$** and **$(Et_2NPh)_2prPMe$** were presented in previous publications [23,24]. The compound **$(Me_2NPh)_2prPNEt$** crystallizes in monoclinic space group *C2/c*. To characterize planarity of this type of molecules, three almost planar fragments **A, B** and **C** (see Supplementary materials) can be considered (Figs. 2, 3). The piperidone ring adopts flattened boat conformation with dihedral angle of C2–N–C6 with plane **A** (C2 → C6) equal to 57.07°.

The bond-length distributions in the conjugated bridges definitely show an alternation of single and double bond lengths. In the aromatic rings we observe bond lengths distribution which indicates its qunoid character (Table S1). The dihedral angle between fragments A and **B** is 12.82° and between fragments **A** and **C** is 19.47°. This deviation from planarity is significantly larger than in case of relative piperidone molecules, presented in Table S3 (see Supplementary .aterials), including two with short alkene chain **$(Et_2NPh)_2PMe$** and **$(Me_2NPh)_2PEt$** [23]. It is possible to see, that the deviation from planarity in the molecules with ethyl substitutes in the phenyl rings is less significant.

2.3. One- and two-photon absorption and fluorescence spectra

OPA, TPA and emission spectra of **$(Me_2NPh)_2prPR^2$** were measured in toluene (Figs. 4a, 5a), while DMF was used for **$(Et_2NPh)_2prPR^2$** compounds for better solubility (Figs. 4b, 5b). Table 1 summarizes photophysical properties of the compounds. TPA cross sections were also measured in chloroform for both **$(Me_2NPh)_2prPR^2$** and **$(Et_2NPh)_2prPR^2$** series, though poor sample stability in chloroform restrain us from quantitative comparison. Nevertheless, **$(Me_2NPh)_2prPR^2$** samples dissolved in chloroform show larger cross sections compared to samples in toluene, which suggests that the cross sections are influenced by solvent polarity (see Fig. 5).

All compounds have the absorption maxima near 500 nm. The maxima of dimethylamino-derivatives, **$(Me_2NPh)_2prPR^2$**, are in the range of 465–475 nm, while the diethylamino-derivatives,

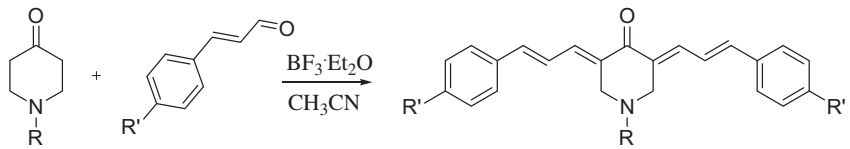

1, 2a,b **3a,b**

R = Me (**1**), Et (**2a**), H·HCl·H_2O (**2b**)

R' = NMe_2 (**3a**), NEt_2 (**3b**)

$(Me_2NPh)_2prPMe$, 93%
$(Et_2NPh)_2prPMe$, 92%
$(Me_2NPh)_2prPEt$, 86%
$(Et_2NPh)_2prPEt$, 90%
$(Me_2NPh)_2prPH$, 88%
$(Et_2NPh)_2prPH$, 91%

Scheme 1.

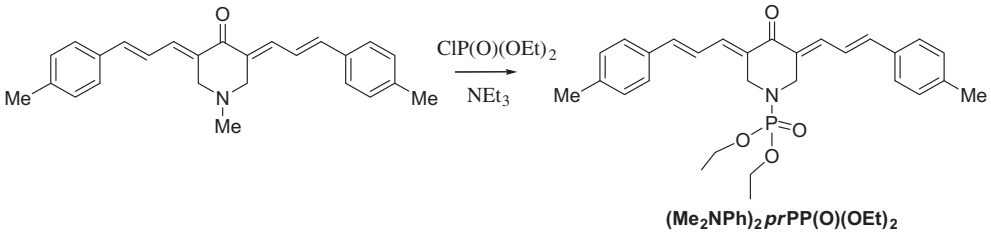

Scheme 2.

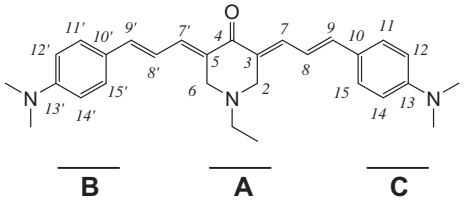

Fig. 2. Planar fragments in 3,5-bisarylidene*propen*piperidin-4-one **(Me$_2$NPh)$_2$*pr*PNEt** molecule.

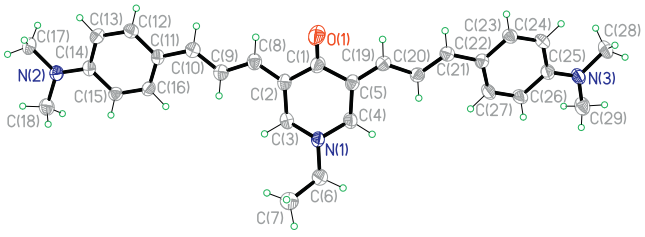

Fig. 3. ORTEP plot of **(Me$_2$NPh)$_2$*pr*PEt** with the numbering scheme in projection on the best plane. Thermal ellipsoids are shown with 50% probability level. Hydrogen atoms are drawn as circles of arbitrary small radii for clarity.

(Et$_2$NPh)$_2$*pr*PR^2, have a slightly red-shifted absorption maxima near 460–500 nm. This slight red-shift is expected because of higher electron donating properties of diethylamino group. Notably the substituent at the piperidone nitrogen atom almost do not affect absorption spectra and extinctions, except for a small red-shift in maximum of the **(Me$_2$NPh)$_2$*pr*PP(O)(OEt)$_2$** compound. The maximum extinction coefficients are all approximately $\sim 6 \times 10^5\ M^{-1}\ cm^{-1}$.

TPA spectra of the **(Me$_2$NPh)$_2$*pr*PR^2** compounds show similar line shapes, independent on the substituents at nitrogen central core atom. The peak cross sections, however, vary in the series, monotonically decreasing as **R^2** goes from H to Me and Et. For the phosphorus-containing sample, though, the peak cross section is almost the same as for the **(Me$_2$NPh)$_2$*pr*PH**. In case of the **(Et$_2$NPh)$_2$*pr*PR^2** samples, the TPA spectra also do not vary with the change of the substituents at the central ring. Their cross sections are larger than that for the **(Me$_2$NPh)$_2$*pr*PR^2** compounds. This observation can be linked with structural characteristic of these molecules, which shows that molecules with ethyl substituents **(Et$_2$NPh)$_2$*pr*PR^2** have greater planarity. The only exception is **(Et$_2$NPh)$_2$*pr*PH**, which has lower cross sections due to lower extinction coefficient value. This lower extinction is most likely an artifact of our measurements as the sample begins to decompose in the solution right away, which results in a reduced value. This decomposition is thought to be due to either sensitivity toward light and polar solvents or possibly free-radical induced oxidation and reduction [25].

As it was stated earlier, our goal was to optimize TPA properties of the previously studied 3,5-bis(arylidene)piperidin-4-ones [20] so as to make them possible candidates for two photon photodynamic therapy. TPA activity of 3,5-bis(arylidene)piperidin-4-ones was measured in between 740 and 860 nm, and the maximum cross-section was found to be ~300 GM [15]. All the **(R^{1}NPh)$_2$*pr*PR^2** compounds showed larger cross sections, and the greatest value, ~1900 GM for **(Et$_2$NPh)$_2$*pr*PEt,** is six times greater than the published values. This cross section value is comparable with porphyrin derivatives used as two-photon sensitizers for TPA laser treatment of mice tumors located on depth of 2 cm [26,27].

Emission spectra of the compounds are shown in Fig. 5. For the **(Me$_2$NPh)$_2$*pr*PR^2** compounds, the emission peak is around 540 nm, except for the phosphorus-containing sample, which is 15 nm red-shifted relative to the other samples, similar to its red-shift in OPA. The **(Et$_2$NPh)$_2$*pr*PR^2** compounds show similar spectra with the peaks at 670 nm. The fluorescence quantum yields are rather low, ranging from 0.05 for **(Et$_2$NPh)$_2$*pr*PH** to 0.12 for **(Me$_2$NPh)$_2$*pr*PP(O)(OEt)$_2$**. The quantum yields are the smallest for the H-substitutients at the central ring and slightly larger for the other substituents.

3. Experimental details

3.1. Materials and general methods

NMR spectra were measured with a Bruker AMX-300 spectrometer using residual proton signals of deuterated solvent as an internal standard (^{1}H, ^{13}C) and H_3PO_4 (^{31}P) as an external standard.

Table 1
Photophysical properties of the synthesized compounds.

Compound	λ_{max}*, nm	ε_{max}*, $M^{-1}cm^{-1}$	λ_{FL}	φ	$\lambda_{TPA,max}$	σ_2, GM
(Me$_2$NPh)$_2$*pr*PH	482	5.60×10^5	550	0.09	810	490
(Me$_2$NPh)$_2$*pr*PMe	484	7.65×10^5	540	0.11	820	450
(Me$_2$NPh)$_2$*pr*PEt	491	5.39×10^5	540	0.10	820	380
(Me$_2$NPh)$_2$*pr*PP(O)(OEt)$_2$	496	6.54×10^5	555	0.12	820	520
(Et$_2$NPh)$_2$*pr*PH	472	3×10^{5}**	675	0.05	890	850**
(Et$_2$NPh)$_2$*pr*PMe	508	5.55×10^5	675	0.07	890	1640
(Et$_2$NPh)$_2$*pr*PEt	503	6.36×10^5	675	0.07	890	1880

* λ_{max} (peak OPA wavelength) and ε_{max} (peak extinction coefficient) are shown in DMF for all compounds.
** (Et$_2$NPh)$_2$*pr*PH tend to decompose in solution, therefore, even when its extinction is measured right after synthesis, it still shows lower value compared to the other compounds.

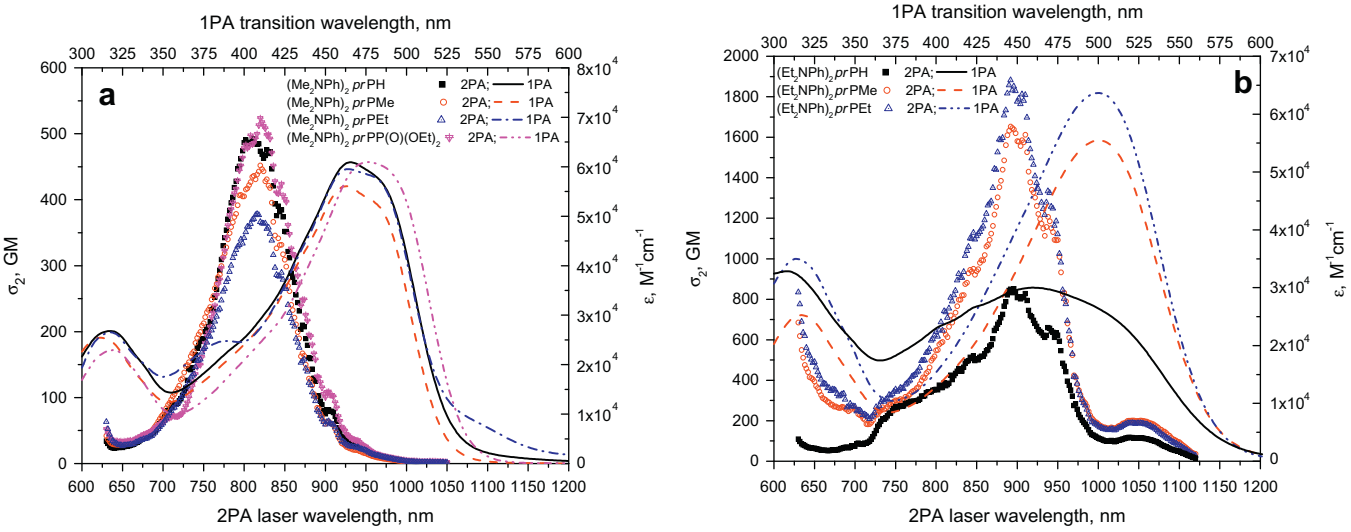

Fig. 4. One-photon (lines) and two-photon absorption spectra of the compounds studied (a) $(Me_2NPh)_2prPR^2$, in toluene, (b) $(Et_2NPh)_2prPR^2$, in DMF.

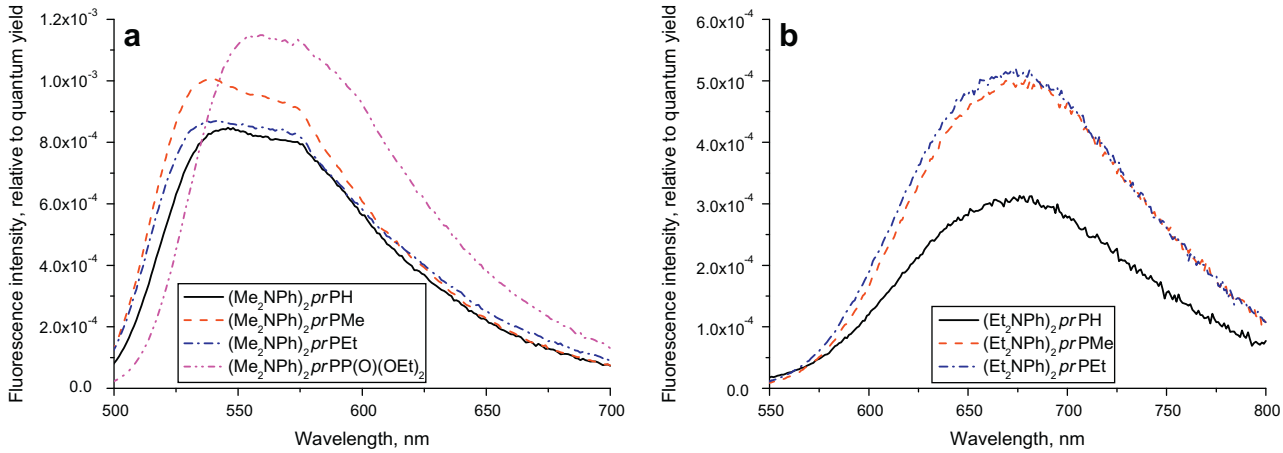

Fig. 5. Emission spectra of the studied compounds: (a) $(Me_2NPh)_2prPR^2$; (b) $(Et_2NPh)_2prPR^2$. Relative to the fluorescence standard Rhodamine 6G, in methanol.

Analytical TLCs were performed with Sorbent Technologies Silica G TLC plates w/UV254. IR spectra were recorded with KBr pellets on a "Magna-IR™" (Nicolet), resolution 6 cm^{-1}, 17 scans. UV spectra were recorded with UV–visible spectrophotometer HP 8452. Fluorescence spectra were recorded with RF-5301PC spectrofluorophotometer Shimadzu. Fluorescence spectra were collected with the excitation wavelength set to 490 nm, and the fluorescence quantum yields were measured relative to Rhodamine 6G.

The TPA spectra of **$(Me_2NPh)_2prPR^2$** in toluene solution and **$(Et_2NPh)_2prPR^2$** in DMF solution were measured over a broad spectral region using a double-arm two-photon-excited fluorescence (2PEF) method [28] relative to Rhodamine 6G in methanol [29]. The 2PA spectra were also measured in chloroform, however, photochemical stability of the samples in this solvent was poor. Freshly prepared samples were excited using vertically polarized light from a tunable femtosecond (fs) optical parametric amplifier (TOPAS-C, Spectra-Physics). The relative 2PEF signal of the sample versus the standard was recorded as a function of excitation wavelength, using 90° detection geometry and an imaging spectrometer (Acton SpectraPro-150). The spectra were scaled to the TPA cross section measured at the selected wavelength of 820 nm, using Rhodamine 6G in methanol as a Ref. [15] for **$(Me_2NPh)_2prPR^2$**, and 950 nm using LDS-698 in chloroform as a Ref. [21] for **$(Et_2NPh)_2prPR^2$**.

Commercial available initial aldehydes **3 a,b** and substituted piperidin-4-ones **1**, **2 a,b** were used without additional purification.

3.2. (3E,5E)-3,5-bis[(2E)-3-(arylidene)prop-2-en-1-ylidene]-1-methylpiperidin-4-one (General procedure)

Boron trifluoride etherate (4 mmol) was added to a solution of the corresponding aldehyde **3 a,b** (2 mmol) and 4-piperidone **1**, **2 a,b** (1 mmol) in 1 mL of CH_3CN. The mixture was keep overnight. After chilling the mixture to ambient temperature, the precipitate was filtered off and recrystallized from MeOH to give the final 3,5-bisarylidene*propen*piperidin-4-ones as a tetrafluoroborate salts. The salts were neutralized with 5% water solution of $NaHCO_3$ by addition of solid material to the above mentioned solution. The obtained precipitates were dried under pressure.

3.3. (3E,5E)-3,5-bis{(2E)-3-[4-(dimethylamino)phenyl]prop-2-en-1-ylidene}-1-methylpiperidin-4-one ($(Me_2NPh)_2prPMe$)

Purple crystalline solid, Mp 194–196 °C. Yield 93%. IR (KBr, n cm^{-1}): 2929, 2896, 2798 (dimethylamino group vibration), 1650 (C=O), 1593 (C=C), 1572, 1519, 1446, 1364, 1327, 1295, 1229, 1189, 1156, 1119, 1086, 1062, 972, 943, 809. ^1H NMR ($CDCl_3$), *d*,

ppm: 2.56 (s, 3H, Me), 3.02 (s, 12H, $2NMe_2$), 3.63 (s, 4H, $_{cyclic}N(CH_2)_2$), 6.68 (d, 4H, $^3J_{HH}$ = 9.1 Hz), 6.73 (d, 1H, $^3J_{HH}$ = 11.9 Hz, CH), 6.78 (d, 1H, $^3J_{HH}$ = 11.9 Hz, CH), 6.93 (d, 2H, $^3J_{HH}$ = 15.3 Hz, CH), 7.41 (d, 4H, $^3J_{HH}$ = 8.9 Hz), 7.48 (d, 2H, $^3J_{HH}$ = 11.5 Hz, CH). High resolution mass spectr, *m*/*z* calc. for $C_{28}H_{33}N_3O$ 428.2702. Found, 428.2707.

3.4. (3E,5E)-3,5-bis{(2E)-3-[4-(diethylamino)phenyl]prop-2-en-1-ylidene}-1-methylpiperidin-4-one ($(Et_2NPh)_2prPMe$)

Purple crystalline solid, Mp 218–220 °C. Yield 92%. IR (KBr, n cm^{-1}): 2970, 2925, 2896 (diethylamino group vibration), 1659 (C=O), 1593 (C=C), 1565, 1524, 1467, 1409, 1373, 1352, 1299, 1266, 1225, 1197, 1156, 1078, 1004, 976, 952, 812. ^{1}H NMR ($CDCl_3$), *d*, ppm: 1.16 (m, 12H, 2 $N(CH_2\underline{CH_3})_2$), 3.14 (s, 3H, Me), 3.25–4.48 (m, 8H, 2 $N(\underline{CH_2}CH_3)_2$), 4.30 (s, 4H, $_{cyclic}N(CH_2)_2$), 6.47 (d, 4H, $^3J_{HH}$ = 9.1 Hz), 6.56–6.69 (m, 2H, CH), 6.98 (d, 2H, $^3J_{HH}$ = 14.7 Hz, CH), 7.29 (d, 4H, $^3J_{HH}$ = 9.4 Hz), 7.62 (d, 2H, $^3J_{HH}$ = 12.1 Hz, CH). High resolution mass spectr, *m*/*z* calc. for $C_{32}H_{41}N_3O$ 484.3328. Found, 484.3338.

3.5. (3E,5E)-3,5-bis{(2E)-3-[4-(dimethylamino)phenyl]prop-2-en-1-ylidene}-1-ethylpiperidin-4-one ($(Me_2NPh)_2prPEt$)

Red crystalline solid, Mp 186–188 °C. Yield 86%. IR (KBr, n cm^{-1}): 2897, 2856, 2803 (dimethylamino group vibration), 1655 (C=O), 1593 (C=C), 1564, 1524, 1478, 1442, 1364, 1328, 1291, 1234, 1185, 1156, 1123, 1087, 1066, 948, 813. ^{1}H NMR ($CDCl_3$), *d*, ppm: 1.27 (t, 3H, $^3J_{HH}$ = 7.2 Hz, $NCH_2\underline{CH_3}$), 2.75–2.85 (m, 2H, $N\underline{CH_2}CH_3$), 3.03 (s, 12H, $2NMe_2$), 3.86 (s, 4H, $_{cyclic}N(CH_2)_2$), 6.68 (d, 4H, $^3J_{HH}$ = 8.9 Hz), 6.73 (d, 1H, $^3J_{HH}$ = 11.9 Hz, CH), 6.78 (d, 1H, $^3J_{HH}$ = 11.9 Hz, CH), 6.97 (d, 2H, $^3J_{HH}$ = 14.9 Hz, CH), 7.42 (d, 4H, $^3J_{HH}$ = 8.9 Hz), 7.55 (d, 2H, $^3J_{HH}$ = 11.7 Hz, CH). ^{13}C NMR (DMSO-d_6), *d*, ppm: 10.69 ($NCH_2\underline{CH_3}$), 40.35 ($2NMe_2$), 51.10 (C^2, C^6), 51.64 ($N\underline{CH_2}CH_3$), 112.18 (C^{12}, C^{14}, $C^{12'}$, $C^{14'}$), 118.26 (C^8, $C^{8'}$), 124.16 (C^9, $C^{9'}$), 129.84 (C^{11}, C^{15}, $C^{11'}$, $C^{15'}$), 131.00 (C^{10}, $C^{10'}$), 144.89 (C^3, C^5), 151.53 (C^7, $C^{7'}$), 154.67 (C^{13}, $C^{13'}$), 193.91 (C^4). High resolution mass spectr, *m*/*z* calc. for $C_{29}H_{35}N_3O$ 442.2858. Found, 442.2858.

3.6. (3E,5E)-3,5-bis{(2E)-3-[4-(diethylamino)phenyl]prop-2-en-1-ylidene}-1-ethylpiperidin-4-one ($(Et_2NPh)_2prPEt$)

Purple crystalline solid, Mp > 300 °C (decomposition). Yield 90%. IR (KBr, n cm^{-1}): 2962, 2929 (diethylamino group vibration), 1650 (C=O), 1626 (C=C), 1597, 1569, 1524, 1401, 1356, 1303, 1262, 1193, 1152, 1115, 980, 956, 813. ^{1}H NMR (DMSO-d_6), *d*, ppm: 1.09 (t, 12H, $^3J_{HH}$ = 7.2 Hz, 2 $N(CH_2\underline{CH_3})_2$), 1.15 (t, 3H, $^3J_{HH}$ = 6.0 Hz, $NCH_2\underline{CH_3}$), 3.34–3.45 (m, 2H, $N\underline{CH_2}CH_3$, $N\underline{CH_2}CH_3$), 4.02 (s, 4H, $_{cyclic}N(CH_2)_2$), 6.64 (d, 4H, $^3J_{HH}$ = 9.0 Hz), 6.84–7.01 (m, 4H, 2CH), 7.22 (d, 4H, $^3J_{HH}$ = 12.0 Hz), 7.45 (d, 4H, $^3J_{HH}$ = 9.0 Hz). ^{13}C NMR (DMSO-d_6), *d*, ppm: 13.11 ($N(CH_2\underline{CH_3})_2$, $NCH_2\underline{CH_3}$), 44.36 ($N(\underline{CH_2}CH_3)_2$), 51.65 ($N\underline{CH_2}CH_3$), 53.37 ($C^2$, C^6), 111.82 (C^{12}, C^{14}, $C^{12'}$, $C^{14'}$), 118.56 (C^8, $C^{8'}$), 123.94 (C^9, $C^{9'}$), 130.03 (C^{11}, C^{15}, $C^{11'}$, $C^{15'}$), 130.59 (C^7, $C^{7'}$), 135.98 (C^{10}, $C^{10'}$), 142.91 (C^3, C^5), 148.80 (C^{13}, $C^{13'}$), 185.43 (C^4). High resolution mass spectr, *m*/*z* calc. for $C_{33}H_{43}N_3O$ 498.3484. Found, 498.3485.

3.7. (3E,5E)-3,5-bis{(2E)-3-[4-(dimethylamino)phenyl]prop-2-en-1-ylidene}piperidin-4-one ($(Me_2NPh)_2prPH$)

Red crystalline solid, Mp > 198 °C (decomposition). Yield 88%. After separation additional purification was used, particularly column chromatography in spectrophotometric grade acetonitrile. Yield (after column) 28%. IR (KBr, n cm^{-1}): 2901, 2807 (dimethylamino group vibration), 1646 (C=O), 1593 (C=C), 1565, 1524, 1475, 1442, 1360, 1324, 1299, 1287, 1229, 1187, 1156, 1123, 1058, 968, 944, 841, 809. ^{1}H NMR ($CDCl_3$), *d*, ppm: 3.02 (s, 12H, $2NMe_2$), 4.01 (s, 4H, $_{cyclic}N(CH_2)_2$), 6.68 (d, 4H, $^3J_{HH}$ = 9.1 Hz), 6.75 (d, 1H, $^3J_{HH}$ = 11.7 Hz, CH), 6.80 (d, 1H, $^3J_{HH}$ = 11.7 Hz, CH), 6.93 (d, 2H, $^3J_{HH}$ = 15.1 Hz, CH), 7.41 (d, 4H, $^3J_{HH}$ = 8.9 Hz), 7.47 (d, 2H, $^3J_{HH}$ = 11.5 Hz, CH). ^{13}C NMR ($CDCl_3$), *d*, ppm: 40.40 ($2NMe_2$), 46.67 (C^2, C^6), 112.20 (C^{12}, C^{14}, $C^{12'}$, $C^{14'}$), 118.56 (C^8, $C^{8'}$), 124.89 (C^9, $C^{9'}$), 128.99 (C^{11}, C^{15}, $C^{11'}$, $C^{15'}$), 131.59 (C^{10}, $C^{10'}$), 136.05 (C^7, $C^{7'}$), 142.63 (C^3, C^5), 151.14 (C^{13}, $C^{13'}$), 186.69 (C^4). High resolution mass spectr, *m*/*z* calc. for $C_{27}H_{31}N_3O$ 414.2545. Found, 414.2548.

3.8. (3E,5E)-3,5-bis{(2E)-3-[4-(diethylamino)phenyl]prop-2-en-1-ylidene}piperidin-4-one ($(Et_2NPh)_2prPH$)

Brown crystalline solid, Mp 174–176 °C. Yield 91%. After separation additional purification was used, particularly column chromatography in spectrophotometric grade acetonitrile. Yield (after column) 34%. IR (KBr, n cm^{-1}): 2970, 2929, 2893 (diethylamino group vibration), 1659 (C=O), 1610 (C=C), 1597, 1565, 1520, 1446, 1397, 1372, 1352, 1299, 1266, 1189, 1152, 1082, 1009, 964, 841, 805. ^{1}H NMR (DMSO-d_6), *d*, ppm: 1.10 (t, 3H, $^3J_{HH}$ = 9.0 - Hz, $NCH_2\underline{CH_3}$), 3.33–3.44 (m, 2H, $N\underline{CH_2}CH_3$), 4.23 (s, 4H, $_{cyclic}N(CH_2)_2$), 6.68 (d, 4H, $^3J_{HH}$ = 8.9 Hz), 6.90 (d, 1H, $^3J_{HH}$ = 11.9 Hz, CH), 6.95 (d, 1H, $^3J_{HH}$ = 11.9 Hz, CH), 7.08 (d, 2H, $^3J_{HH}$ = 14.9 Hz, CH), 7.38 (d, 2H, $^3J_{HH}$ = 12.0 Hz, CH), 7.42 (d, 4H, $^3J_{HH}$ = 9.0 Hz). High resolution mass spectr, *m*/*z* calc. for $C_{31}H_{39}N_3O$ 470.3171. Found, 470.3186.

3.9. Diethyl ((3E,5E)-3,5-bis{(2E)-3-[4-(dimethylamino)phenyl]prop-2-en-1-ylidene}-4-oxopiperidin-4-one ($(Me_2NPh)_2prPP(O)(OEt)_2$)

To a mixture of the corresponding 3,5-bis{(2E)-3-[4-(dimethylamino)phenyl]prop-2-en-1-ylidene}piperidin-4-one **$(Me_2NPh)_2$*prPH*** (0.9 mmol) and triethylamine (2.2 mmol) in dry tetrahydrofuran (7 ml) a solution of corresponding chlorophosphate (1.8 mmol) in dry tetrahydrofuran (3 ml) was added. The reaction mixture was stirred at room temperature for over 5 h. The course of reaction was monitored by TLC or NMR as appropriate. After completion of the reaction, the mixture was evaporated at reduced pressure, dissolved in CH_2Cl_2 and washed with water. The organic layer was separated, evaporated at reduced pressure and purified by column chromatography on SiO_2 (THF as an eluent). The appropriate fractions were evaporated under reduced pressure to give the final product. Brown crystalline solid was obtained, Mp > 350 °C (decomposition). Yield 65%. IR (KBr, n cm^{-1}): 2382, 2341, 2292 (diethylamino group vibration), 1740, 1732, 1699 (C=O), 1687 (C=C), 1655, 1622, 1597, 1573, 1544, 1519, 1393, 1364, 1287, 1225, 1176, 1152, 1103, 968, 944, 833, 801. ^{1}H NMR ($CDCl_3$), *d*, ppm: 1.17 (t, 6H, $^3J_{HH}$ = 7.0 Hz, $^4J_{HP}$ = 0.8 Hz, $P(O)(OCH_2\underline{CH_3})_2$), 2.96 (s, 12H, $2NMe_2$), 3.78–3.96 (m, 4H, $P(O)(O\underline{CH_2}$-$CH_3)_2$), 4.26 (d, $^3J_{HP}$ = 9.3 Hz, 4H, $_{cyclic}N(CH_2)_2$), 6.70 (d, 4H, $^3J_{HH}$ = 9.1 - Hz), 6.88 (d, 1H, $^3J_{HH}$ = 11.7 Hz, CH), 6.93 (d, 1H, $^3J_{HH}$ = 11.5 Hz, CH), 7.04 (d, 2H, $^3J_{HH}$ = 15.1 Hz, CH), 7.27 (d, 2H, $^3J_{HH}$ = 11.7 Hz, CH), 7.51 (d, 4H, $^3J_{HH}$ = 9.1 Hz). ^{31}P NMR ($CDCl_3$), *d*, ppm: 8.11. High resolution mass spectr, *m*/*z* calc. for $C_{31}H_{40}N_3O_4P$ 550.2835. Found, 550.2826.

3.10. Crystallographic determination

The X-ray diffraction experiment was performed using a Bruker SMART APEX II CCD diffractometer; Mo Kα radiation (λ = 0.71073 Å) at 100 K. The raw data frames were integrated with the SAINT + program using narrow-frame algorithm [30]. Absorption corrections were applied using the semiempirical method of the SADABS program [31]. The structure was solved by direct methods and refined using the Bruker SHELXTL programs suite [32] by full-matrix least-squares methods on F^2 with *SHELXL-97* in anisotropic approximation for all non-hydrogen atoms. All H

Table 2
Crystallographic data for **(Me_2NPh)$_2$*pr*PEt**.

Empirical formula	$C_{29}H_{35}N_3O$
Formula weight	441.60
Crystal system	Monoclinic
Space group	C_2/c
a, Å	16.858(4)
b, Å	9.888(2)
c, Å	30.483(10)
α, deg.	90
β, deg.	100.551(6)
γ, deg.	90
V, Å^3	4995(2)
Z	8
ρ_{calc}, g/cm^3	1.174
GOF on F^2	1013
R_1, ωR_2 ($I > 2\sigma(I)$)	0.0553, 0.1175
R_1, ωR_2 (all data)	0.1177, 0.1474

atoms were placed in idealized positions and refined with constrained C—H distances and *U*iso(H) values set to be 1.2*U*eq or 1.5*U*eq (for methyl group) of the attached C atom. Crystallographic data have been deposited with the Cambridge Crystallographic Data Centre as supplementary publication No. CCDC 902708. Copies of the data can be obtained, free of charge, on application to CCDC, 12 Union Road, Cambridge CB2 1EZ, UK (fax: +44 (0)1223 336033 or e-mail: deposit@ccdc.cam.ac.uk). Details of X-ray experiment and structure solution are presented in Table 2.

4. Conclusions

A series of 3,5-bisarylidene*propen*piperidin-4-one compounds, with general formula – **(R^1Ph)$_2$*pr*PR^2** – with different substitutes at the central nitrogen atom and at the aryl rings was synthesized. According to obtained spectroscopic data two compounds, **(Et_2NPh)$_2$*pr*PMe**, and **(Et_2NPh)$_2$*pr*PEt** demonstrated the best two-photon absorption properties in the studied range. Practical applications of investigated TPA materials require additional studies which we plan to conduct in future.

Acknowledgments

This work was supported by the NSF DMR-0934121 and CHE-0820852. The authors are grateful for this support. We thank Dr. Michail Makarov and Prof. Dr. Irina L. Odinets for valuable discussion.

Appendix A. Supplementary material

^{1}H, ^{13}C NMR spectra for **(R^1Ph)$_2$*pr*PR^2** (R^1 = NEt_2, NMe_2; R^2 = H, Me, Et, P(O)$(OEt)_2$), Tables 1S–3S, summarizing the geometrical parameters obtained from the X-ray data. Supplementary data associated with this article can be found, in the online version, at http://dx.doi.org/10.1016/j.molstruc.2012.12.034.

References

[1] C.A. Mosley, D.C. Liotta, J.P. Snyder, Highly active anticancer curcumin analogues, in: Bharat B. Aggarwal, Young-Joon Surh, Shishir Shishodia (Eds.), The Molecular Targets and Therapeutic uses of Curcumin in Health and Disease, Springer, New York, NY, 2007, pp. 77–105.
[2] J.R. Dimmock, N.M. Kandepu, M. Hetherington, J.W. Quail, U. Pugazhenthi, A.M. Sudom, M. Chamankhah, P. Rose, E. Pass, T.M. Allen, S. Halleran, J. Szydlowski, B. Mutus, M. Tannous, E.K. Manavathu, T.G. Myers, E. De Clercq, J. Balzarini, J. Med. Chem. 41 (1998) 1014.
[3] D.A. Koechel, E.J. Cafruny, J. Med. Chem. 16 (1973) 1147.
[4] J.R. Fry, J.H. Fentem, A. Salim, S.P.A. Tang, M.J. Garle, D.A. Whiting, J. Pharm. Pharmacol. 45 (1993) 166.
[5] J. Traber, M. Suter, P. Walter, C. Richter, Biochem. Pharmacol. 43 (1992) 961.
[6] U. Das, J. Alcorn, A. Shrivastav, R.K. Sharma, E. De Clercq, J. Balzarini, J.R. Dimmock, J. Med. Chem. 42 (2007) 71.
[7] J.R. Dimmock, P. Kumar, A.J. Nazarali, N.L. Motaganahalli, T.P. Kowalchuk, M.A. Beazely, J.W. Quail, E.O. Oloo, T.M. Allen, J. Szydowski, E. De Clercq, J. Balzarini, Eur. J. Med. Chem. 35 (2000) 967–977.
[8] J.R. Dimmock, U. Das, H.I. Gul, M. Kawase, H. Sakagami, Z. Baráth, I. Ocsovsky, J. Molnár, Bioorg. Med. Chem. Lett. 15 (2005) 1633.
[9] J.L. Wike-Hooley, A.P. van den Berg, J. van der Zee, H.S. Reinhold, Eur. J. Cancer Clin. Oncol. 21 (1985) 785.
[10] J.R. Dimmock, V.K. Arora, M.J. Duffy, R.S. Reid, T.M. Allen, G.Y. Kao, Drug Des. Discov. 8 (1992) 291.
[11] H.I. El-Subbagh, S.M. Abu-Zaid, M.A. Mahran, F.A. Badria, A.M. Al-Obaid, J. Med. Chem. 43 (2000) 2915.
[12] C. Jobin, C.A. Bradham, M.P. Russi, B. Juma, A.S. Narula, D.A. Brenner, R.B. Sartor, J. Immunol. 163 (1999) 3474.
[13] S. Kumar, U. Narain, K. Misra, Bioconjugate Chem. 12 (2001) 464.
[14] N. Ahmad, S.K. Katiyar, H. Mukhtar, in: J. Thiele, P. Elsner (Eds.), Oxidants and Antioxidants in Cutaneous Biology, KARGER, Jena, 2001, pp. 128–139.
[15] K.W. Short, T.L. Kinnibrugh, D.M. Sammeth, T.V. Timofeeva, Kessel 7164 (2009) 716411.
[16] G. Kodis, V. Gulbinas, L. Valkunas, S. Jursenas, Adv. Mater. Opt. Electron. 6 (1996) 391.
[17] X. Zhou, A.-M. Ren, J.-K. Feng, X.-J. Liu, J. Mol. Struct. 679 (2004) 157.
[18] V.A. Shakin, Sh. Abe, Phys. Rev. B50 (1994) 4306.
[19] M. Drobizhev, A. Karotki, Yu. Dzenis, A. Rebane, J. Phys. Chem. B 107 (2003) 7540.
[20] E.A. Badaeva, T.V. Timofeeva, A.S. Musanov, S. Treriak, J. Phys. Chem. A 109 (2005) 7276.
[21] E.S. Leonova, M.V. Makarov, E.Yu. Rybalkina, T.V. Timofeeva, I.L. Odinets, Eur. J. Med. Chem. 45 (2010) 992.
[22] M.V. Makarov, E.Yu. Rybalkina, G.-V. Röschenthaler, K.W. Short, T.V. Timofeeva, I.L. Odinets, Eur. J. Med. Chem. 44 (2009) 2135.
[23] V.N. Nesterov, L.N. Zakharov, S.S. Sarkisov, M.J. Curleyd, A. Urbase, Acta Cryst. C64 (2008) o73.
[24] V.N. Nesterov, T.V. Timofeeva, S.S. Sarkisov, A. Leyderman, Ch.Y.-C. Leed, M.Yu. Antipin, Acta Cryst. C59 (2003) o605.
[25] S.Z. Vatsadze, M.A. Manaenkova, N.V. Sviridenkova, N.V. Zyk, D.P. Krut'ko, A.V. Churakov, M.Yu. Antipin, J.A.K. Howard, H. Lang, Russ. Chem. Bull. 55 (2006) 1184.
[26] J.R. Starkey, A.K. Rebane, M.A. Drobizhev, F. Meng, A. Gong, A. Elliott, K. McInnerney, Ch.W. Spangler, Clin. Cancer Res. 14 (2008) 6564.
[27] M. Drobizhev, F. Meng, A. Rebane, Y. Stepanenko, E. Nickel, Ch.W. Spangler, J. Phys. Chem. B 110 (2006) 9802.
[28] N.S. Makarov, J. Campo, J.M. Hales, J.W. Perry, Opt. Mater. Exp. 1 (2011) 551.
[29] N.S. Makarov, M. Drobizhev, A. Rebane, Opt. Exp. 16 (2008) 4029.
[30] SAINT+, Version 6.2a; Bruker Analytical X-ray System, Inc., Madison, WI, 2001.
[31] SADABS; Bruker Analytical X-ray System, Inc.: Madison, WI (1999).
[32] SHELXTL, Version 6.10; Bruker Analytical X-ray System, Inc., Madison, WI, 1997.